JOURNAL OF SPACECRAFT AND ROCKETS
Vol. 43, No. 4, July–August 2006

# Sensitivity Analysis for Rapid Prototyping of Entry Vehicles

Scott Josselyn* and I. Michael Ross†
*Naval Postgraduate School, Monterey, California 93943*

**A procedure is presented for the application of parameter value-function analysis to the problem of rapid prototyping of entry vehicles. The trajectory optimization problem is imbedded in a family of canonically parameterized optimal control problems. Rather than repeatedly solving an ensemble of trajectory optimization problems, it is shown that a combination of sensitivity- and covector mapping theorems can be easily exploited to gauge quickly the effect of a parameter on the performance of the entry vehicle. Although the theory is not limited to the type or number of parameters, the ideas are demonstrated with three design variables: the maximum heating rate on the vehicle, the parasitic drag coefficient, and the vehicle mass. No change in the proposed method is necessary to carry out a similar analysis for other plant parameters for additional purposes such as the design of robust guidance algorithms. With use of the Legendre pseudospectral method and results from nonsmooth analysis, it is shown how to validate the sensitivity results.**

## Nomenclature

| | | |
|---|---|---|
| $A$ | = | reference area, ft$^2$ |
| $a$ | = | aerodynamic acceleration, ft/s$^2$ |
| $C$ | = | heating rate coefficient, Btu $\cdot$ s$^{2.07}$ $\cdot$ ft$^{3.57}$ $\cdot$ slug$^{0.5}$ |
| $C_D$ | = | drag coefficient |
| $C_L$ | = | lift coefficient |
| $D$ | = | drag, lb |
| $J$ | = | generic cost functional |
| $\mathcal{L}$ | = | lift, lb |
| $m$ | = | vehicle mass, slug |
| $\boldsymbol{p}$ | = | generic parameter vector |
| $q$ | = | heating rate |
| $\bar{q}$ | = | dynamic pressure |
| $R_0$ | = | reference radius, ft |
| $r$ | = | radial position, ft |
| $\boldsymbol{u}$ | = | control vector |
| $v$ | = | speed, ft/s |
| $\boldsymbol{x}$ | = | state vector |
| $\alpha$ | = | angle of attack, deg |
| $\beta$ | = | inverse scale height, ft$^{-1}$ |
| $\gamma$ | = | flight-path angle, deg |
| $\delta$ | = | bank angle, deg |
| $\partial_p$ | = | proximal subdifferential |
| $\theta$ | = | longitude, $^\circ$ |
| $\boldsymbol{\lambda}$ | = | Lagrange multiplier |
| $\mu$ | = | Earth gravitational constant, ft$^3$/s$^2$ |
| $\rho$ | = | atmospheric density, slug/ft$^3$ |
| $\phi$ | = | latitude, $^\circ$ |
| $\psi$ | = | heading angle, deg |
| $\Omega$ | = | angular velocity of Earth, deg/s |

*Subscripts*

| | | |
|---|---|---|
| $f$ | = | final condition |
| $n, s, w$ | = | normal, tangential, and binormal directions |
| 0 | = | initial or nominal condition |

Received 13 July 2003; presented as Paper 2003-5500 at the AIAA Guidance, Navigation, and Control Conference, Austin, TX, 11–14 August 2003; revision received 7 January 2004; accepted for publication 9 January 2004. 

*Graduate Student, Department of Aeronautics and Astronautics; josselynsb@navair.navy.mil. Student Member AIAA.

†Associate Professor, Department of Mechanical and Astronautical Engineering; imross@nps.navy.mil. Associate Fellow AIAA.

## Introduction

ONE of the long-standing problems in both military and commercial space is the problem of access to space. Roughly speaking, for commercial space, it is the problem of inexpensive access to space, whereas for the military, it is assured access. Although new technologies are being explored to meet these challenges, it is apparent that to reduce development costs of the various possibilities, new tools are necessary to assess quickly the quantitative impact of the design variables on the performance of the space transportation system. Furthermore, in appraising the overall cost of the design, it is also important to estimate the degradation in performance due to aging components. Once the vehicle is designed, additional parameter analysis is necessary to assist the design of robust guidance algorithms. It is necessary to use high-order nonlinear models and a unified approach to harness the full scope of the trade space of space transportation systems, because they are highly nonlinear and strongly coupled with respect to many parameters.

In this paper, we propose a rapid and efficient approach to perform a parameter value-function analysis for such studies in conjunction with rapid trajectory optimization. Our approach is based on combining sensitivity theorems[1–4] with a covector mapping theorem.[5–7] Roughly speaking, sensitivity theorems provide a relationship between a change in a desired variable to changes in the parameters. Whereas such theorems are well developed in finite-dimensional optimization problems,[1] sensitivity theorems are much less developed in optimal control problems.[8] This is, in part, because of the regularity assumptions necessary to develop second-order optimality conditions.[9] To use these theorems properly, it is necessary to verify numerically all of the intricate conditions.[8] This step involves an accurate solution to the adjoint equations associated with the optimal control problem.

A standard method to find the costates associated with the optimal control problem is to solve the two-point boundary-value problem that arises as a result of the application of the minimum principle.[10] This problem is numerically sensitive to single-shooting methods due to the ill-conditioned transition matrices of the perturbed system. Multiple-shooting methods significantly alleviate this problem and have been effectively used to solve a number of problems.[8,11] These so-called indirect (shooting) methods are used because direct methods, which are significantly easier to use, typically do not provide accurate (in the sense of optimality) solutions[6,12]; hence, the verification process becomes questionable (with direct methods). The gap between direct and indirect methods can be closed by way of closure conditions,[6,7] which essentially render closable direct methods equivalent to indirect methods, thus, resolving the accuracy problem. A covector mapping theorem[6,7] then provides accurate costate information without the burden of solving the two-point-boundary-value problem. This facilitates a rapid sensitivity

analysis for complex optimal control problems, which is the method adopted in this paper.

In this paper, we are mainly concerned with the sensitivity of the cost function to variations in the design parameters. Deferring the details and limitations of our approach, we note that the concept of rapid trajectory optimization (a necessary but not sufficient condition for efficient sensitivity analysis) concomitantly solves a number of other important problems such as that of minimizing the turn-around time for mission replanning and the design of the outer loop of an adaptive two-degree-of-freedom guidance system.[13,14] In addition, the concept of sensitivity analysis automatically implies a verification technique for the optimality of proposed trajectory designs and a means to design optimal robust guidance algorithms that are insensitive with respect to environmental disturbance, for example, atmospheric models, and vehicle models, for example, inertia dyadic. In other words, the problem addressed in this paper is a fundamental one associated with the rapid prototyping of advanced entry vehicles.

## Entry Dynamic Model

We demonstrate the ideas by arbitrarily choosing a particular set of coordinates that describe the state of the vehicle by the six-dimensional vector $\boldsymbol{x} = (r, \theta, \phi, v, \psi, \gamma)$ consisting of its radial position, longitude, latitude, speed, heading angle, and flight-path angle, respectively. The equations of motion are given by[15]

$$\dot{r} = v \sin\gamma \tag{1}$$

$$\dot{\theta} = \frac{v \cos\gamma \cos\psi}{r \cos\phi} \tag{2}$$

$$\dot{\phi} = \frac{v \cos\gamma \sin\psi}{r} \tag{3}$$

$$\dot{v} = a_s - g(r)\sin\gamma + \Omega^2 r \cos\phi(\sin\gamma\cos\phi - \cos\gamma\sin\phi\sin\psi) \tag{4}$$

$$\dot{\psi} = \frac{a_w}{v\cos\gamma} - \frac{v}{r}\cos\gamma\cos\psi\tan\phi - \frac{\Omega^2 r}{v\cos\gamma}\sin\phi\cos\phi\cos\psi + 2\Omega(\tan\gamma\cos\phi\sin\psi - \sin\phi) \tag{5}$$

$$\dot{\gamma} = \frac{a_n - g(r)\cos\gamma}{v} + \frac{v\cos\gamma}{r} + \frac{\Omega^2 r}{v}\cos\phi(\cos\gamma\cos\phi + \sin\gamma\sin\phi\sin\psi) + 2\Omega\cos\phi\cos\psi \tag{6}$$

where $g(r) = \mu/r^2$ is the inverse-square gravitational acceleration. The aerodynamic accelerations, $a_s$, $a_n$, and $a_w$, resolved in the tangential, normal, and binormal directions are

$$a_s = -D/m, \qquad a_n = L\cos\delta/m, \qquad a_w = L\sin\delta/m \tag{7}$$

where $m$ is the mass of the vehicle. The aerodynamic lift and drag forces are given by

$$L = \bar{q}AC_L(\alpha), \qquad D = \bar{q}AC_D(\alpha) \tag{8}$$

where

$$\bar{q} = \tfrac{1}{2}\rho(r)v^2 \tag{9}$$

and $\rho(r)$ is the exponentially varying atmospheric density,

$$\rho(r) = \rho_0 e^{-\beta(r - R_0)} \tag{10}$$

The lift and drag coefficients are modeled as

$$C_L(\alpha) = C_{L_0} + C_{L_\alpha}\alpha \tag{11}$$

$$C_D(\alpha) = C_{D_0} + C_{D_\alpha}\alpha + C_{D_{\alpha 2}}\alpha^2 \tag{12}$$

## Nominal Problem Formulation

Suppose that the cross-range performance is a key design parameter. For an initial equatorial orbit, maximizing the cross range is equivalent to maximizing or minimizing the final latitude. Thus, the problem is to find a control history, $t \mapsto \boldsymbol{u} = (\delta, \alpha)$, that minimizes (or maximizes) the final latitude:

$$J[\boldsymbol{x}(\cdot), \boldsymbol{u}(\cdot), t_f; \boldsymbol{p}] = \phi(t_f) \tag{13}$$

subject to the dynamic model of the preceding section and the heating rate constraint

$$q(r, v, \alpha) \le q_{\max} \tag{14}$$

where the heating rate function, $q(r, v, \alpha)$, adapted from Ref. 12, is given by

$$q(r, v, \alpha) = q_a(\alpha) q_r(r, v) \tag{15}$$

where

$$q_a = h_0 + h_1\alpha + h_2\alpha^2 + h_3\alpha^3, \qquad q_r = C\rho^N(r)v^M \tag{16}$$

and $\boldsymbol{p} = \boldsymbol{p}_0$ is the nominal parameter vector (data) for the problem. The nominal data for the problem are adapted from Ref. 12 and provided in Table 1 consistent with the notations used in this paper. (The unit for $\alpha$ is radian.) The boundary conditions (also part of $\boldsymbol{p}_0$) are summarized in Table 2.

Now suppose that the heat load on the vehicle was the prime driver for design optimization. In this case, we may take the cost function to be

$$J[\boldsymbol{x}(\cdot), \boldsymbol{u}(\cdot), t_f; \boldsymbol{p}] = \int_{t_0}^{t_f} q[r(t), v(t), \alpha(t)]\,\mathrm{d}t \tag{17}$$

and use $\phi(t_f)$ as a target parameter, that is, make it part of the boundary conditions. Similarly, other options are possible. For the

**Table 1 Nominal data adapted from Ref. 12**

| Parameter | Value |
|---|---|
| $A$ | 2,690 ft$^2$ |
| $C$ | $9.289 \times 10^{-9}$ Btu $\cdot$ s$^{2.07}$ $\cdot$ ft$^{3.57}$ $\cdot$ slug$^{0.5}$ |
| $C_{L_0}$ | −0.2070 |
| $C_{L_\alpha}$ | 1.676 |
| $C_{D_0}$ | 0.07854 |
| $C_{D_\alpha}$ | −0.3529 |
| $C_{D_{\alpha 2}}$ | 2.040 |
| $h_0$ | 1.067 |
| $h_1$ | −1.101 |
| $h_2$ | 0.6988 |
| $h_3$ | −0.1903 |
| $m$ | 7,008 slug |
| $M$ | 3.07 |
| $N$ | 0.5 |
| $q_{\max}$ | 100 Btu $\cdot$ ft$^2$/s |
| $R_0$ | 20,902,900 ft |
| $\beta$ | $4.20168 \times 10^{-5}$/ft |
| $\rho_0$ | 0.002378 slug/ft$^3$ |
| $\mu$ | $1.4076\,539 \times 10^{16}$ ft$^3$/s$^2$ |
| $\Omega$ | $7.2722 \times 10^{-5}$/s |

**Table 2 Nominal boundary conditions**

| Parameter | Value |
|---|---|
| $r_0 - R_0$ | 260,000 ft |
| $\theta_0$ | 0 |
| $\phi_0$ | 0 |
| $v_0$ | 25,600 ft/s |
| $\psi_0$ | 0 |
| $\gamma_0$ | −1.0 deg |
| $r_f - R_0$ | 80,000 ft |
| $v_f$ | 2,500 ft/s |
| $\gamma_f$ | −5 deg |

purposes of clarity, we limit the scope of this paper to cross-range maximization.

## Imbedding the Nominal Problem

In all, this problem has 29 parameters with nominal values given in Tables 1 and 2. Roughly speaking, the parameters at the top of Table 1 are vehicle design parameters, whereas those at the bottom of Table 1 are environmental model parameters. For example, the maximum allowable heating rate represents one of many model parameters that can be related to the mass of the thermal protection system. The vehicle mass $m$ may be classified as either a design parameter or a guidance parameter because it undergoes a potentially large discontinuous change from its nominal value depending on the cargo and crew onboard. In Table 2, all of the initial conditions are collected to form a set of navigation parameters, whereas the final conditions are the target parameters for a terminal area energy management. Denoting these 29 parameters as $\boldsymbol{p} \in \mathbb{R}^{29}$, with nominal value $\boldsymbol{p} = \boldsymbol{p}_0$ as specified in Tables 1 and 2, we define the parameter value function to be

$$V(\boldsymbol{p}) := \min_{\{x(\cdot),u(\cdot),t_f\}} J[\boldsymbol{x}(\cdot), \boldsymbol{u}(\cdot), t_f; \boldsymbol{p}] \tag{18}$$

Hence, $V(\boldsymbol{p}_0)$ is the optimal cost function (cross range) for this entry problem at the nominal value, that is, the problem posed in the last section. To determine the effect of these parameters on the cost function, a brute force approach would be to solve an ensemble of trajectory optimization problems over all $\boldsymbol{p} \in \mathcal{P}$, where $\mathcal{P} \subseteq \mathbb{R}^{29}$ denotes the constraint set of possible variations in all 29 parameters listed earlier. It is clear that not only is this a laborious task, but it creates additional problems even if this arduous exercise was carried out. For example, how does one analyze the effect of 29 parameters? One possible approach would be to pick them out one by one and analyze the effect of each parameter separately. This approach is somewhat justified if one assumes that each parameter has an uncoupled effect on the cost function. Obviously, this is not true for this problem (and for most nonlinear problems). Hence, a systematic approach is quite essential to perform trade space studies and explore various concepts. This is known as parameter value-function analysis[2,3] and is described next.

## Parameter Value Function Analysis

Consider the trivial finite-dimensional optimization problem: minimize

$$V(\boldsymbol{p})$$

subject to

$$\boldsymbol{p} - \boldsymbol{p}_0 = \boldsymbol{0} \tag{19}$$

which is a special case of a canonical parameterization.[2] Then, according to the sensitivity theorem,[2–4] we have

$$\boldsymbol{\lambda}_p \in \partial_p V(\boldsymbol{p}_0) \tag{20}$$

where $\partial_p V(\boldsymbol{p}_0)$ is the proximal subdifferential[2–4] of the value function at the point $\boldsymbol{p} = \boldsymbol{p}_0$ and $\boldsymbol{\lambda}_p$ is the Lagrange multiplier associated with the trivial constraint, $\boldsymbol{p} - \boldsymbol{p}_0 = \boldsymbol{0}$. The proximal subdifferential is the set of all proximal subgradients. A proximal subgradient is the slope of a parabola that approximates $V$ from below. Hence, a proximal subdifferential generalizes the standard approximation of a differentiable function by tangent lines to a set-valued representation. This generalization facilitates a nonsmooth calculus in such a manner that it reduces to standard calculus when the functions of interest are differentiable. See Refs. 2–4 for further details. Thus, if $V(\boldsymbol{p})$ is differentiable at $\boldsymbol{p}_0$, we have

$$\boldsymbol{\lambda}_p = \frac{\partial V}{\partial \boldsymbol{p}} \tag{21}$$

The reason Eq. (21) cannot be used in general is that the parameter value function is typically nondifferentiable. In fact, no amount of smoothness imposed on the nominal trajectory optimization problem will render the value function smooth. Under mild conditions, the value function is Lipschitz continuous (see Refs. 2–4). Because a Lipschitz-continuous function is differentiable almost everywhere, Eq. (21) can be used in the following manner: Solve problem (19). If Eq. (21) is valid at the point $\boldsymbol{p} = \boldsymbol{p}_0$, then the equation of the tangent plane of the surface defined by the value function at the point $\boldsymbol{p}_0$ is given by

$$V_{T_0}(\boldsymbol{p}) = V(\boldsymbol{p}_0) + \boldsymbol{\lambda}_{p_0}^T(\boldsymbol{p} - \boldsymbol{p}_0) \tag{22}$$

Now pick another point close to $\boldsymbol{p}_0$, for example, $\boldsymbol{p}_1$. This point may be arbitrarily chosen, or along the direction of steepest ascent or descent, $\boldsymbol{p}_1 = \boldsymbol{p}_0 \pm \varepsilon \boldsymbol{\lambda}_{p_0}$, $\varepsilon > 0$, or guided by the physics of the problem. In any case, we solve Eq. (19) again at the fixed value of $\boldsymbol{p} = \boldsymbol{p}_1$. If Eq. (21) is valid, then the equation to the tangent plane at the new point $\boldsymbol{p}_1$ is given by

$$V_{T_1}(\boldsymbol{p}) = V(\boldsymbol{p}_1) + \boldsymbol{\lambda}_{p_1}^T(\boldsymbol{p} - \boldsymbol{p}_1) \tag{23}$$

In the next step, we compare, $|V_{T_0}(\boldsymbol{p}_1) - V(\boldsymbol{p}_1)|$ and $|V_{T_1}(\boldsymbol{p}_0) - V(\boldsymbol{p}_0)|$. If these errors are small and about the same value, then the assumption of differentiability was justified, and we immediately have the sensitivity information for further study and analysis (such as determining which parameter changes yields the maximum payoff). In the case when both of these errors are large, it means that both these points were nondifferentiable (perhaps the direction $\boldsymbol{p}_0 - \boldsymbol{p}_1$ was some ridge or crevice of the value function) and Eqs. (22) and (23) were supporting hyperplanes and not tangent planes. To move away from these points of nondifferentiability, one can then repeat the exercise for another point $\boldsymbol{p}_2$ that is orthogonal to $\boldsymbol{p}_0 - \boldsymbol{p}_1$. As noted earlier, if the value function is Lipschitz (as we expect it to be most of the time), then the described procedure is not expected to generate wild error norms. In any case, it is apparent that we may map out the value function and be able to find a point of differentiability quickly at some $\varepsilon$ neighborhood of $\boldsymbol{p}_0$.

Note that the trivial finite-dimensional optimization problem posed as problem (19) is equivalent to the nontrivial infinite dimensional optimization problem posed as problem (18) with $\boldsymbol{p} = \boldsymbol{p}_0$. Hence, the outlined method requires that the optimal control problem be solved accurately and rapidly and that the solution set include accurate values of the covector functions, that is, Lagrange multiplier functions for the infinite-dimensional problem. Because accuracy is critical to performing a sensitivity analysis, it is necessary to pick an accurate dynamic optimization method. The conventional wisdom[12] on accuracy is an indirect method. However, indirect methods come with all of the trappings outlined in Ref. 12. Thus, it is apparent that if one could solve the trajectory optimization problem with the ease of a direct method but the accuracy of an indirect method, rapid parameter analysis could be carried out. Unfortunately, most direct methods do not tie the resulting solutions to the minimum principle; hence a two-step direct–indirect approach is frequently promulgated to find the sensitivity multipliers and covector functions associated with the extremal solutions. One major drawback of the direct–indirect approach is that a significant amount of labor is still necessary to derive all of the necessary conditions, including complex switching and junction conditions. In the preliminary design phases, new constraints are added or old ones removed rather frequently. This means that the necessary conditions have to be rederived repeatedly, thus, subverting rapid analysis. Even if these tasks were somehow performed rapidly, solving the multipoint-boundary-value problem is a fundamentally elaborate project.

Over the past few years, efficient and accurate methods have been developed to solve complex trajectory optimization problems. The Legendre pseudospectral method[7,16] is a particularly effective method that has been used, by way of the DIDO software package,[17] to solve a vast number[13,18–24] of complex problems. In addition to efficiency, DIDO provides spectrally accurate solutions for the costates and other covectors without the use of any analytical differential equations for the adjoints and the derivation of the necessary conditions. This is made possible by an implementation of the covector mapping theorem (CMT).[6,7] This key theorem can be visualized as shown in Fig. 1. Here, $B$ represents any optimal control problem, the superscript $N$ represents the discretization, and the superscript $\lambda$

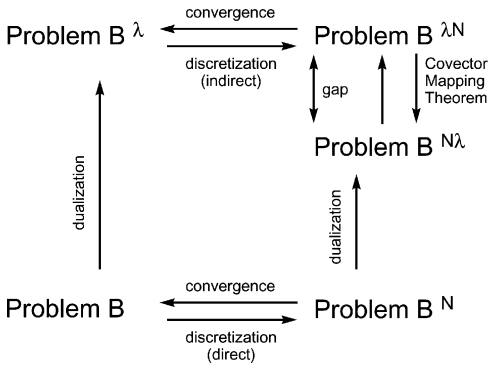


**Fig. 1 Schematic for CMT (from Ref. 7.)**

represents the dualization, that is, the problem generated by an application of the necessary conditions. In general terms, the CMT ties the Karush–Kuhn–Tucker (KKT) multipliers of the finite-dimensional optimization problem to the discrete covector functions by closing the gap generated by the noncommutative operations of discretization and dualization. In other words, the path taken in Fig. 1 going horizontal first and vertical afterward is not commutative with going vertical first and horizontal afterward. What the CMT does is facilitate a means to close the gap as indicated. Hence, from the KKT multipliers, one can find covector functions to spectral accuracy, that is, all of the multipliers can be obtained as if one solved the problem by an indirect Legendre pseudospectral method. A readable discussion of this concept as a fundamental principle in optimal control, with applications well beyond the pseudospectral method, is presented in Ref. 6. Clearly, one main advantage of the CMT is that it obviates the need for a two-tier direct–indirect method and provides a rapid approach to value function analysis. A recent application of this approach to the problem of rapid trajectory optimization for entry vehicles is described in Ref. 18.

## Results and Analysis

We now apply value-function analysis to the problem of entry trajectory and design optimization. We demonstrate how our method can be used for predicting the deviation in vehicle performance with respect to deviations in the design parameters. Our method can also be used for a number of other purposes as outlined in the Introduction, but we limit the scope of the paper to perturbations in the design parameters.

The imbedded family of entry problems is solved using DIDO,[17] which implements many of the recent advances in the Legendre pseudospectral method (see Refs. 7 and 13) that include an automatic sparsity pattern generation and exploitation of the discrete Jacobian sparsity by way of the nonlinear programming solver SNOPT.[25] To use DIDO, no knowledge of pseudospectral methods is necessary. The optimal control problem is coded in much the same way as one writes it down, thanks to the era of object-oriented software. Following the technique described in Ref. 18, feasibility is declared when the state histories obtained by a Runge–Kutta-propagation (ode45 routine in MATLAB® that implements the Dormand–Prince pair) of the initial conditions using the interpolated controls obtained from DIDO match the states (obtained from DIDO) within a prescribed tolerance. Convergence is declared when DIDO controls match the extremal controls (within some prescribed tolerance) computed through an application of the CMT.

To illustrate our procedure in a tutorial manner, we limit our discussions to the three parameters associated with the design of the vehicle: maximum heating rate $q_{\max}$, parasitic drag coefficient $C_{D_0}$, and mass $m$; thus, we have

$$\boldsymbol{p} = \left[q_{\max}, C_{D_0}, m\right]^T \tag{24}$$

The nominal values are as stipulated in Table 1 and reproduced here for quick reference where the units are the same as in Table 1:

$$\boldsymbol{p}_0 = [100, 0.07854, 7008]^T \tag{25}$$

The extension of the method to the 29 parameters identified in Tables 1 and 2 is almost trivial, as will be apparent shortly.

For the nominal run [of maximizing cross range, $V(\boldsymbol{p}_0) =$ maximum $\phi(t_f)$], DIDO generates the sensitivity multiplier

$$\boldsymbol{\lambda}_p = \begin{pmatrix} 2.180 \times 10^{-4} \\ -5.791 \\ -1.877 \times 10^{-6} \end{pmatrix} \tag{26}$$

Because of the large variations in the scales of the nominal parameters [Eq. (25)], this vector is more meaningful when the effect of units on the parameters is removed because what matters is not the actual values of the components of $\boldsymbol{\lambda}_p$ but the product, $\boldsymbol{\lambda}_p^T \boldsymbol{p}_0$ [Eq. (22)],

$$\boldsymbol{\lambda}_p^T \boldsymbol{p}_0 = \underbrace{\lambda_{q_{\max}} q_{\max}}_{0.02180} + \underbrace{\lambda_{C_{D_0}} C_{D_0}}_{-0.4548} + \underbrace{\lambda_m m}_{-0.01316} \tag{27}$$

Assuming that Eq. (21) is a correct interpretation of the multipliers, we get

$$\text{maximum } \phi|_{p_0 + dp} = \text{maximum } \phi|_{p_0} + \mathrm{d}V \tag{28}$$

where

$$\mathrm{d}V = \lambda_{q_{\max}} \mathrm{d}q_{\max} + \lambda_{C_{D_0}} \mathrm{d}C_{D_0} + \lambda_m \, \mathrm{d}m \tag{29}$$

Hence, the numbers in Eq. (27) reveal that the parasitic drag coefficient is the most sensitive parameter to the maximum value of the cross range, whereas the vehicle mass offers the least sensitivity. Quantitatively, the parasitic drag coefficient offers about 35 times higher sensitivity [from $(\lambda_{C_{D_0}} C_{D_0})/(\lambda_m m)$] to the maximum value of the cross range than the vehicle mass. Similarly, the cross range is about two times more sensitive [from $(\lambda_{q_{\max}} q_{\max})/(\lambda_m m)$] to the maximum allowable heating rate than the vehicle mass. The signs on the components of the multiplier reveals the directions of their effects: If a larger cross range is desired, the maximum allowable heating rate must be increased, while the parasitic drag coefficient and mass must be decreased. From Eq. (22), we can also determine the change in the maximum value of the cross range to a first-order accuracy [assuming the interpretation of Eq. (21)]. The maximum value of the cross range in degrees obtained from DIDO was

$$V(\boldsymbol{p}_0) = 36.87 \tag{30}$$

Thus, a 10% change in all of the parameters (in the plus direction for $q_{\max}$ and minus direction for the other parameters) is predicted to change the maximum value of the cross range in degrees to

$$V_{T_0}(\boldsymbol{p}_1) = 39.68 \tag{31}$$

with the maximum contribution of the change (equal to 2.60 deg) coming from a change in the parasitic drag coefficient. All of this analysis is valid only under the interpretation of Eq. (21). A validation of the foregoing analysis around this nominal point can easily be done by changing the parameters by 10% and resolving problem (19). When this 10% point is denoted as $\boldsymbol{p}_1$, DIDO generates (in degrees)

$$V(\boldsymbol{p}_1) = 39.88 \tag{32}$$

Because $|V_{T_0}(\boldsymbol{p}_1) - V(\boldsymbol{p}_1)| = 0.20$ deg is small (in the sense of engineering judgement), we can conclude the result to be validated. However, our method offers a better validation by examining the new sensitivity multiplier at point $\boldsymbol{p}_1$:

$$\boldsymbol{\lambda}_p = \begin{pmatrix} 7.407 \times 10^{-5} \\ -7.062 \\ -1.105 \times 10^{-6} \end{pmatrix} \tag{33}$$

Proceeding backward to our original point along this new hyperplane [Eq. (23)], we get a predicted drop in the cross range (in degrees) to be

$$V_{T_1}(\boldsymbol{p}_0) = 36.62 \tag{34}$$

Because $|V_{T_1}(\boldsymbol{p}_0) - V(\boldsymbol{p}_0)| = 0.25$ deg, that is, the movement along the hyperplanes generates the same errors (to the first decimal place), we conclude that the hyperplanes were tangent planes, thus, validating the results.

It is apparent that such analyses carry over to any number of parameters, that is, it is irrelevant whether $\boldsymbol{p} \in \mathbb{R}^3$ or $\boldsymbol{p} \in \mathbb{R}^{29}$. Regardless, it is instructive to visualize the parameter value function in some sense. Because $\boldsymbol{p} \in \mathbb{R}^3$, the surface described by $\boldsymbol{p} \mapsto V$ is in $\mathbb{R}^4$. Hence, it is necessary to further restrict $\boldsymbol{p}$ to $\mathbb{R}^2$ to visualize the value function in $\mathbb{R}^3$. By choosing to plot the parameter Value function for the pairs of parameters, $(q_{\max}, C_{D_0})$, $(C_{D_0}, m)$, and $(m, q_{\max})$ at the nominal values of the remaining third parameter, we essentially obtain the orthogonal projections of the three-dimensional surface in $\mathbb{R}^4$ as a two-dimensional surface in $\mathbb{R}^3$ at the nominal point. Clearly such projectional plots can be performed for $\boldsymbol{p} \in \mathbb{R}^{29}$ as well, except that we will now have 812 plots. Hence, the differential–geometric method described is more suited for parameter analysis greater than two. Needless to say, it is still instructive to examine certain two-dimensional surfaces.

Figure 2 shows a sectional projection of the parameter value function onto the $(q_{\max}, C_{D_0})$ plane. The dark pane is the plane obtained from sensitivity analysis. The dots in Fig. 2 correspond to the repeat (and rapid) solutions to problem (19) and, hence, represent the true values of the value function. The sectional surface is a triangle-based cubic approximation of the data, generated automatically in MATLAB by griddata. The dark plane is the projection of the hyperplane obtained from Eq. (22). From Fig. 2, it is apparent that the value function is locally smooth and that Eq. (22) indeed represents the tangent plane at the nominal point. This notion is further amplified in Figs. 3 and 4, where the surface of Fig. 2 is projected onto the $q_{\max}$ and $C_{D_0}$ axes, respectively, along with the plane (now a line in $\mathbb{R}^2$). The dashed line in Fig. 3 is the normal to the vector, $(\lambda_{q_{\max}}, -1)$, at the nominal point. Likewise, the dashed line in Fig. 4 is the normal to the vector, $(\lambda_{C_{D_0}}, -1)$, at the nominal point. Results identical to Figs. 3 and 4 were also obtained by restricting $\boldsymbol{p}$ to the single parameter in question. This validates the notion that Figs. 3 and 4 remain unchanged whether $\boldsymbol{p} \in \mathbb{R}$ or $\boldsymbol{p} \in \mathbb{R}^{29}$, an immediate consequence of the fact that the parameters were assumed to be independent in the model. Obviously, if the parameters are dependent and modeled accordingly, then the parameter space would be smaller. Because integrating models across various disciplines is often semianalytical, it is apparent that a sensitivity analysis is quite useful in a systems engineering setting so that the results obtained by an apparent independence of the various parameters can be checked with experts in the relevant fields. In any event, Figs. 3 and 4 also illustrate that the sensitivity multipliers obtained from DIDO do indeed provide equations for the tangent plane when the parameter value function is locally smooth. Figures 5 and 6 represent the projections of the value function on the remaining two directions as indicated. The dark pane is the plane obtained from sensitivity analysis. Note that care must be taken in interpreting the sensitivity multipliers in taking into account the units of the parameters and their associated scaling factors.

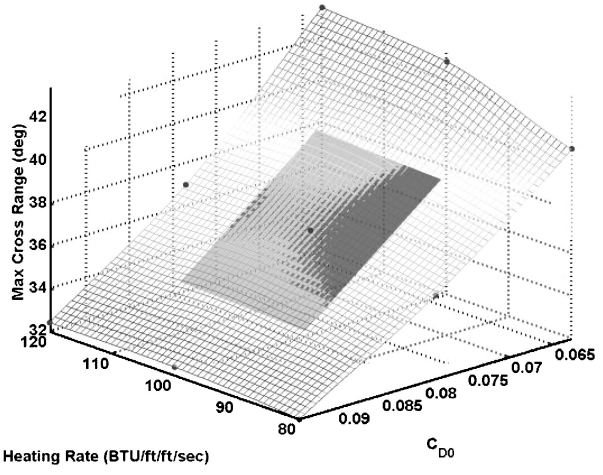


**Fig. 2 Sectional projection of the parameter value function onto the $(q_{\max}, C_{D_0})$ plane at the nominal value of $m$.**

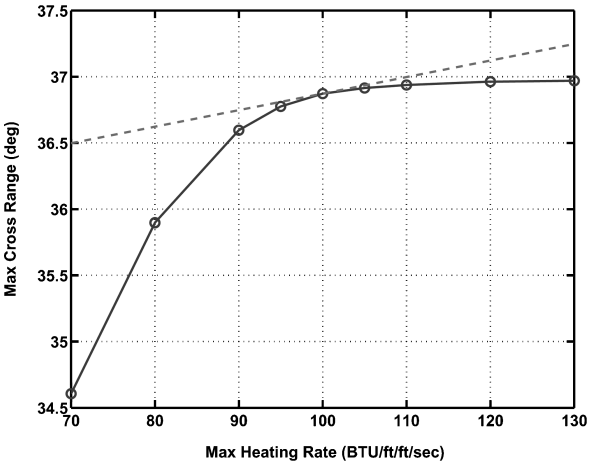


**Fig. 3 Orthogonal projection of the parameter value function onto the $q_{\max}$ axis at the nominal values of $C_{D_0}$ and $m$.**

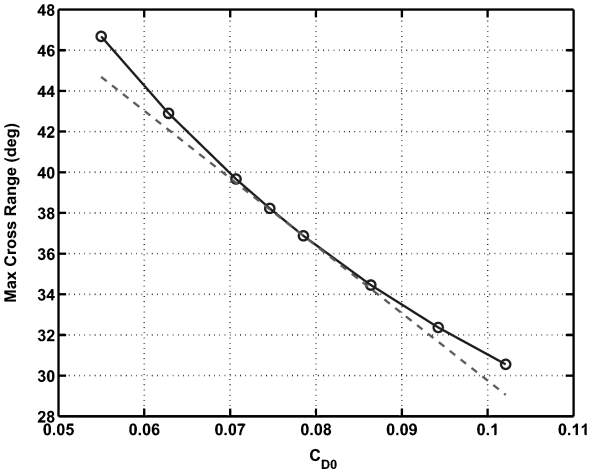


**Fig. 4 Orthogonal projection of the parameter value function onto the $C_{D_0}$ axis at the nominal values of $q_{\max}$ and $m$.**

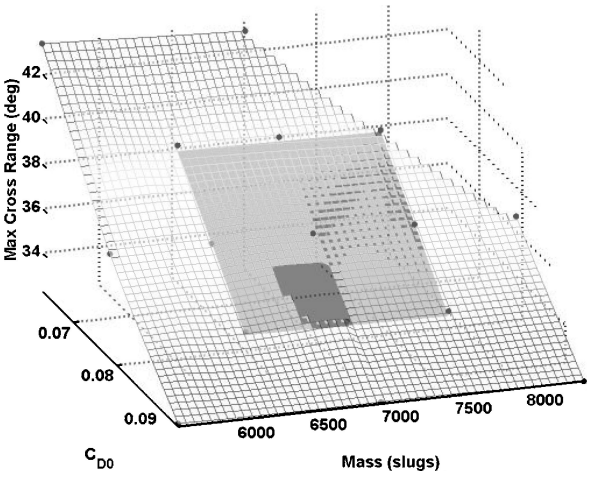


**Fig. 5 Sectional projection of the parameter value function onto the $(C_{D_0}, m)$ plane at the nominal value of $q_{\max}$.**

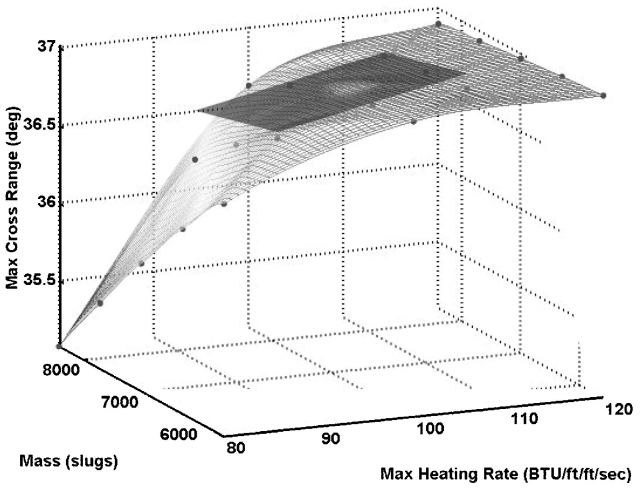


**Fig. 6 Sectional projection of the parameter value function onto the $(m, q_{\max})$ plane at the nominal value of $C_{D_0}$.**

The technique presented here may also be used onboard to gauge the effect of various parameters either during failure of certain components or of inaccurate navigation information. This is because each of these runs can be performed in a matter of seconds to minutes[18] with current technology in both hardware and software. Significantly faster computations are possible with the same hardware simply by exploiting new implementations.[13,26]

## Conclusions

The application of sensitivity theorems in conjunction with the CMT facilitates a rapid procedure for a sensitivity analysis for entry vehicles. This obviates a need for the labor-intensive single-tier indirect method or a two-tier direct–indirect method. Computational time for the entry problem reveals that results can be obtained within a few minutes for high accuracy and less than a minute for reduced accuracy. A further reduction in computational time is possible with current technology and is the subject of ongoing research and implementation.

## References

[1]Fiacco, A. V., *Introduction to Sensitivity and Stability Analysis in Nonlinear Programming*, Academic Press, New York, 1983.

[2]Rockafellar, R. T., "Lagrange Multipliers and Optimality," *SIAM Review*, Vol. 35, No. 2, 1993, pp. 183–238.

[3]Clarke, F. H., Ledayaev, Yu. S., Stern, R. J., and Wolenski, P. R., *Nonsmooth Analysis in Control Theory*, Springer-Verlag, New York, 1998.

[4]Vinter, R. B., *Optimal Control*, Birkhäuser, Boston, 2000.

[5]Ross, I. M., and Fahroo, F, "Convergence of Pseudospectral Approximations for Optimal Control Problems," *Proceedings of the 2001 IEEE Conference on Decision and Control*, Inst. of Electrical and Electronics Engineers, Piscataway, NJ, 2001.

[6]Ross, I. M., and Fahroo, F., "A Perspective on Methods for Trajectory Optimization," AIAA Paper 2002-4727, Aug. 2002.

[7]Ross, I. M., and Fahroo, F., "Legendre Pseudospectral Approximations of Optimal Control Problems," *Lecture Notes in Control and Information Sciences*, Vol. 295, Springer-Verlag, New York, 2003, pp. 327–342.

[8]Malanowski, K., and Maurer, H., "Sensitivity Analysis for State-Constrained Optimal Control Problems," *Discrete and Continuous Dynamical Systems*, No. 4, 1998, pp. 241–272.

[9]Dontchev, A. L., and Hager, W. W., "Lipschitzian Stability for State Constrained Nonlinear Optimal Control," *SIAM Journal on Control and Optimization*, Vol. 36, No. 2, 1998, pp. 698–718.

[10]Bryson, A. E., and Ho, Y. C., *Applied Optimal Control*, Hemisphere, New York, 1975.

[11]Maurer, H., and Pesch, H. J., "Solution Differentiability for Parameteric Nonlinear Control Problems," *SIAM Journal on Control and Optimization*, Vol. 32, No. 6, 1994, pp. 1542–1554.

[12]Betts, J. T., *Practical Methods for Optimal Control Using Nonlinear Programming*, SIAM Advances in Control and Design Series, Society for Industrial and Applied Mathematics, Philadelphia, 2001.

[13]Strizzi, J., Ross, I. M., and Fahroo, F., "Towards Real-Time Computation of Optimal Controls for Nonlinear Systems," AIAA Paper 2002-4945, Aug. 2002.

[14]Yan, H., Fahroo, F., and Ross, I. M., "Real-Time Computation of Neighboring Optimal Control Laws," AIAA Paper 2002-4657, Aug. 2002.

[15]Vinh, N. X., *Optimal Trajectories in Atmospheric Flight*, Elsevier, New York, 1981.

[16]Fahroo, F., and Ross, I. M., "Second Look at Approximating Differential Inclusions," *Journal of Guidance, Control, and Dynamics*, Vol. 24, No. 1, 2001, pp. 131–133.

[17]Ross, I. M., and Fahroo, F., "User's Manual for DIDO 2002: A MATLAB Application Package for Dynamic Optimization," Dept. of Aeronautics and Astronautics, Naval Postgraduate School, NPS Technical Rept., AA-02-002, Monterey, CA, June 2002.

[18]Josselyn, S., and Ross, I. M., "A Rapid Verification Method for the Trajectory Optimization of Reentry Vehicles," *Journal of Guidance, Control, and Dynamics*, Vol. 26, No. 3, 2003, pp. 505–508.

[19]Lu, P., Sun, H., and Tsai, B., "Closed-Loop Endoatmospheric Ascent Guidance," *Journal of Guidance, Control, and Dynamics*, Vol. 26, No. 2, 2003, pp. 283–294.

[20]Melton, R. G., "Comparison of Direct Optimization Methods Applied to Solar Sail Problems," AIAA Paper 2002-4728, Aug. 2002.

[21]Ross, I. M., King, J. T., and Fahroo, F., "Designing Optimal Spacecraft Formations," AIAA Paper 2002-4635, Aug. 2002.

[22]Rea, J., "Launch Vehicle Trajectoy Optimization Using a Legendre Pseudospectral Method," AIAA Paper 2003-5640, Aug. 2003.

[23]Ross, I. M., and Fahroo, F., "Pseudospectral Knotting Methods for Solving Optimal Control Problems," *Journal of Guidance, Control, and Dynamics*, Vol. 27, No. 3, 2004, pp. 397–405.

[24]Infeld, S., and Murray, W., "Optimization of Stationkeeping for a Libration Point Mission," American Astronautical Society, AAS Paper 04-150, Feb. 2004.

[25]Gill, P. E., Murray, W., and Saunders, M. A., "SNOPT: An SQP Algorithm for Large-Scale Constrained Optimization," Dept. of Mathematics, Numerical Analysis Rept. 97-1, Univ. of California, La Jolla, CA, Nov. 1997.

[26]Ross, I. M., and Fahroo, F., "A Unified Computational Framework for Real-Time Optimal Control," *Proceedings of the 2003 IEEE Conference on Decision and Control*, Inst. of Electrical and Electronics Engineers, 2003.

C. Kluever
*Associate Editor*